FREQUENCY RESPONSE ANALYSIS OF HIGHER ORDER COMPOSITE SANDWICH BEAMS WITH VISCOELASTIC CORE[*]

H. ARVIN

Department of Mechanical Engineering, College of Engineering, Boroujen Branch, Islamic Azad University, Boroujen, I. R. of Iran
Email: h.arvin@iauboroujen.ac.ir

Abstract– In this paper, the Hamilton's principle is implemented to derive the coupled partial differential equations of motion of composite sandwich beams with viscoelastic core. The sandwich beams model is based on the higher order theory for composite sandwich beams with viscoelastic core, which regards independent transverse displacements for the face sheets with linear variations along the depth of the core. The core Young's modulus and the beam rotary inertia effects are also taken into account. Frequency response analysis is examined by applying the Galerkin discretization approach on the adimensional equations of motion. The results are validated by comparison with the existing literature. An interesting study is managed for the frequency response sensitivity analysis to the core shear modulus variation. The novelty of this work, besides the study of the fiber angle effects on the frequency response, is finding more logical relationships for regarding or discarding the core Young's modulus and the beam rotary inertia contributions, during the frequency response analysis of the beam. The results indicate the significant role of the core Young's modulus and the beam rotary inertia effects on the frequency response of the beam. The outcomes illustrate regarding the core Young's modulus, contribution hardens the structure while consideration of the beam rotary inertia softens the structure.

Keywords– Sandwich beam, composite structures, viscoelastic core, frequency response, passive control

1. INTRODUCTION

Composite materials are used frequently in aerospace and marine structures due to their high strength/weight ratios and different desirable features achieved by the variation in fiber angles. On the other hand, vibration control of structures, i.e. suppression of the vibration amplitude, protects structures from experiencing fracture and high strains and stresses in large amplitude vibrations, hence, control of the vibration has a significant role in the safety and durability of the structures. Viscoelastic materials are employed frequently for passive vibration control. Therefore, study on the dynamic and vibration characteristics of composite sandwich beams with viscoelastic core (CSBVC), plays a prominent role in research, design and engineering purposes.

A large number of the previous researches on the sandwich structures have implemented the *Mead and Markus* theory (MMT) assumptions [1] to determine the equations of motion. Shakeri et al. [2] studied the dynamic analysis of an axisymmetric cross-ply laminated shallow panel subjected to thermal load using the Galerkin discretization approach. Yim et al. [3] examined the damping behavior of 0° laminated CSBVC. Their study demonstrated the significant effects of the core thickness and the beam length on the loss factors. Pourtakdoust and Fazelzadeh [4] implemented the Galerkin projection approach to investigate the effect of structural damping on the chaotic behavior of nonlinear panels. Cai et al. [5] presented the frequency response analysis of isotropic beams with a passive constrained layer damping,

using the assumed modes method. Zhang and Chen [6] studied the effects of damping of face sheets fibers, fiber angles and viscoelastic core position on the loss factors and natural frequencies of CSBVC, modeled by ANSYS 7.0.

To eliminate the shortage of the assumptions of the MMT, Douglas and Yang [7] presented a model in which they considered the independent transverse displacements for the face sheets of CSBVC. Frostig and Baruch [8] presented a model for linear free vibration analysis of sandwich beams with a flexible core based on a general, higher order theory in which the nonlinear displacement distribution through the depth of the core was considered. Marur and Kant [9] proposed higher order refined displacement models for the free vibration analysis of sandwich beams. Chen and Chan [10] developed a model based on the linear variation of the transverse displacement through the depth of sandwich beams with isotropic face sheets and viscoelastic core. They used an integral finite element method for the frequency response examination.

For improving the other MMT assumptions, Douglas [11] developed his previous research [7] by considering rotary inertia and shear deformation effects of the face sheets. Johnson [12] and Austin [13] revealed that the MMT assumptions are only applicable for sandwich beams with weak cores. Arvin et al. [14] developed a higher order theory for CSBVC by considering linear variation for the transverse displacements of the face sheets through the depth of the beam. They also considered the core Young's modulus and rotary inertia effects. Afshin et al. [15] employed the high-order theory of sandwich structures for examination of the vibration analysis of composite cylindrical sandwich panels containing a viscoelastic core. Damanpack and Khalili [16] investigated the free vibration features of three-layered symmetric sandwich beam using dynamic stiffness method, and employing numerical techniques and the Wittrick-Williams algorithm. Venkatachalam et al. [17] implemented a semi-analytical finite element method to study the effects of an electric field for the electro-rheological fluid material and a magnetic field for the magneto-rheological fluid material on the vibration behavior of the mild steel sandwich shaft disc system.

In this paper, the higher order theory for CSBVC, proposed in [14], is implemented for study on the frequency response of CSBVC. The model was managed for improving the MMT assumptions for sandwich beams. The Hamilton's principle is used to derive the four coupled partial differential equations of motion for the upper and lower face sheets transverse and axial motions of a CSBVC carrying an external transverse load at its upper face sheet. The non-dimensional parameters are introduced to determine the adimensional forms of the equations of motion. The Galerkin discretization approach is applied on the non-dimensional equations of motion for frequency response examination. The face sheets fiber angle effects, and face sheets and core thicknesses influences on the frequency response are investigated. The frequency response sensitivity to the core shear modulus and the fiber angle effects variations is also examined.

2. EQUATIONS OF MOTION

A clamped-free sandwich beam with a viscoelastic core and composite face sheets is depicted in Fig. 1. h_1, h_3 and h_2 are, respectively, the upper and lower face sheets and the core thicknesses and L is the beam length. The x axis is considered along the beam length, while the z axis is considered along the depth of the beam, with the origin at the beam root in the core neutral axis.
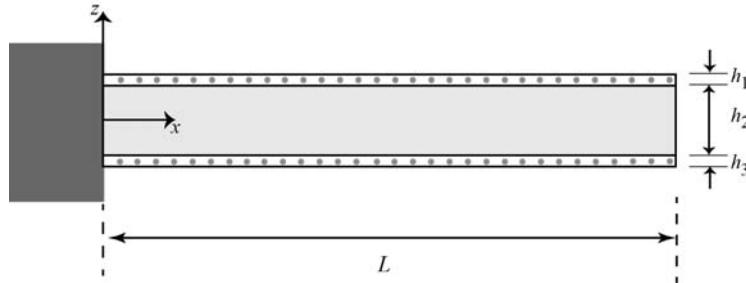
Fig. 1. A schematic of a clamped-free sandwich beam with a viscoelastic
core and composite face sheets

The formulation is based on the higher order theory, which was addressed firstly for the composite sandwich beams in [14]. In agreement with [14], the following assumptions, for improving the MMT assumptions deficiencies, are considered here; I- *Face sheets have independent transverse displacements with linear variation along the core depth*, II- *Contributions of the core Young's modulus are considered in the formulation*, III- *Isotropic materials are replaced with the composite materials at the face sheets*, and IV- *The beam rotary inertia and longitudinal kinetic energy of the core are included*.

Consideration of the aforementioned assumptions in the formulation delivers the kinetic and strain energies [14]. On the other hand, the virtual work, δW_{nc}, performed by the external force acted on the upper face sheet, $f_1(x,t)$, is given by [18]:

$$\delta W_{nc} = \int_0^L f_1(x,t)\ \delta w_1(x,t)\,dx \qquad (1)$$

where, $\delta w_1(x,t)$ is the upper face sheet virtual transverse displacement. In the case of a harmonic tip point transverse load we have $f_1(x,t) = f_0 \delta(x-L)\, e^{i\omega t}$ in which f_0 is the load amplitude and ω is the excitation circular frequency. Thereafter, employing the Hamilton's principle [18] leads to:

$$\int_{t_1}^{t_2} [\,\delta L + \delta W_{nc}\,]dt = 0 \qquad (2)$$

where, $L = T - V$ is the Lagrangian and T is the kinetic energy of the composite sandwich beam introduced in [14]. $V = V_1 + V_2 + V_3$ is the strain energy of the composite sandwich beam, in which V_1, V_3 and V_2 are, respectively, the upper and lower face sheets and the core strain energies denoted in [14]. Subsequently, simplifying the Hamilton's principle yields in four coupled partial differential equations of motion, for the upper and lower face sheets transverse and axial motions, respectively, as:

$$
\begin{aligned}
&\breve{m}_1\ddot{w}_1 + \breve{m}_{21}[\ddot{w}_3 + 1/4h_1h_3\ddot{w}_3'' - 1/2h_1\ddot{u}_3'] - \breve{J}_1\ddot{w}_1'' - 1/2\breve{m}_{22}h_1\ddot{u}_1' + (\bar{Q}_{11}^{(1)}I_1 + Q_{11}A_2h_1^2/16 + Q_{11}I_2h_1^2/ \\
&(4h_2^2))w_1^{(IV)} + Q_{11}(-A_2/16 + I_2/(4h_2^2))h_1h_3w_3^{(IV)} + Q_{11}(1/8A_2 + I_2/(2h_2^2))h_1u_1''' + Q_{11}(1/8A_2 - I_2/ \\
&(2h_2^2))h_1u_3''' + (Q_{13}h_1A_2/2 - Q_{55}(h_1+h_2)^2A_2/(4h_2) - Q_{55}I_2/h_2)/h_2w_1'' + (-1/2Q_{13}(h_1+h_3)A_2/2 - \\
&Q_{55}(h_1+h_2)(h_3+h_2)A_2/(4h_2) + Q_{55}I_2/h_2)/h_2w_3'' + (Q_{13} - Q_{55}(h_1+h_2)/h_2)A_2/(2h_2)u_1' + (Q_{13} + \\
&Q_{55}(h_1+h_2)/h_2)A_2/(2h_2)u_3' + Q_{33}A_2(w_1 - w_3)/h_2^2 = f_1(x,t)
\end{aligned} \qquad (3)
$$

$$
\begin{aligned}
&\breve{m}_3\ddot{w}_3 + \breve{m}_{21}[\ddot{w}_1 + 1/4h_1h_3\ddot{w}_1'' + 1/2h_3\ddot{u}_1'] - \breve{J}_3\ddot{w}_3'' + 1/2\breve{m}_{22}h_3\ddot{u}_3' + (\bar{Q}_{11}^{(3)}I_3 + Q_{11}A_2h_3^2/16 + Q_{11}I_2h_3^2/ \\
&(4h_2^2))w_3^{(IV)} + Q_{11}(-A_2/4 + I_2/h_2^2)h_1h_3/4w_1^{(IV)} + Q_{11}(-1/4A_2 + I_2/h_2^2)h_3/2u_1''' - Q_{11}(1/4A_2 + I_2/ \\
&h_2^2)h_3/2u_3''' + (Q_{13}h_3A_2/2 - Q_{55}(h_3+h_2)^2A_2/(4h_2) - Q_{55}I_2/h_2)/h_2w_3'' + (-1/2Q_{13}(h_1+h_3)A_2/2 - \\
&Q_{55}(h_1+h_2)(h_3+h_2)A_2/(4h_2) + Q_{55}I_2/h_2)/h_2w_1'' - (Q_{13} + Q_{55}(h_3+h_2)/h_2)A_2/(2h_2)u_1' + (-Q_{13} + \\
&Q_{55}(h_3+h_2)/h_2)A_2/(2h_2)u_3' + Q_{33}A_2(w_3 - w_1)/h_2^2 = 0
\end{aligned} \qquad (4)
$$

and

$$\tilde{m}_1\ddot{u}_1 + \tilde{m}_{21}[\ddot{u}_3 - 1/2h_1\ddot{w}_3'] + 1/2\tilde{m}_{22}h_1\ddot{w}_1' - (\breve{Q}_{11}^{(1)}A_1 + Q_{11}(1/4A_2 + I_2/h_2^2))u_1'' + Q_{11}(-1/4A_2 + I_2/h_2^2)u_3''$$
$$-1/2Q_{11}(h_1(1/4A_2 + I_2/h_2^2)w_1''' + h_3(-1/4A_2 + I_2/h_2^2)w_3''') + Q_{55}A_2(u_1 - u_3)/h_2^2 + (-Q_{13} + Q_{55}(h_1 + h_2)) \quad (5)$$
$$/h_2)A_2/(2h_2)w_1' + (Q_{13} + Q_{55}(h_3 + h_2))/h_2)A_2/(2h_2)w_3' = 0$$

$$\tilde{m}_3\ddot{u}_3 + \tilde{m}_{21}[\ddot{u}_1 + 1/2h_3\ddot{w}_1'] - 1/2\tilde{m}_{22}h_3\ddot{w}_3' - (\breve{Q}_{11}^{(3)}A_3 + Q_{11}(1/4A_2 + I_2/h_2^2))u_3'' + Q_{11}(-1/4A_2 + I_2/h_2^2)u_1''$$
$$+1/2Q_{11}(h_3(1/4A_2 + I_2/h_2^2)w_3''' + h_1(-1/4A_2 + I_2/h_2^2)w_1''') + Q_{55}A_2(u_3 - u_1)/h_2^2 + (Q_{13} - Q_{55}(h_3 + h_2)) \quad (6)$$
$$/h_2)A_2/(2h_2)w_3' - (Q_{13} + Q_{55}(h_1 + h_2))/h_2)A_2/(2h_2)w_1' = 0$$

where $\breve{J}_i = (J_i + 1/16m_2h_i^2 + 1/4J_2h_i^2/h_2^2)$, $\tilde{m}_i = (m_i + m_2/4 + J_2/h_2^2)$, $\tilde{m}_{21} = (1/4m_2 - J_2/h_2^2)$ and $\tilde{m}_{22} = (J_2/h_2^2 + 1/4m_2)$. $\breve{Q}_{11}^{(1)}$ and $\breve{Q}_{11}^{(3)}$ are, respectively, the modified reduced stiffness coefficients of the upper and lower face sheets and Q_{ij} are the core stiffness coefficients. $A_i = bh_i$ in which A_i and b are, respectively, the cross section of the *i*th layer of the beam and the beam width; $m_i = \rho_i A_i$ in which m_i and ρ_i are, respectively, the *i*th layer mass per unit length and the corresponding density and $I_i = bh_i^3/12$ and $J_i = \rho_i I_i$ are, respectively, the *i*th layer area and mass moments of inertia. In addition, $w_1(x,t)$, $u_1(x,t)$, $w_3(x,t)$, and $u_3(x,t)$ are, respectively, the transverse and axial displacements of the neutral axis of the upper and lower face sheets.

3. SOLUTION PROCESS

a) Non-dimensionalization of the equations of motion

Due to the generalization of the solution, the following non-dimensional parameters are taken into account:

$$\hat{x} = x/L, \quad \hat{t} = t/T, \quad \hat{w}_i = w_i/h_t, \hat{u}_i = u_i/h_t, \eta = L/h_t, I_{ii} = I_i/(A_t h_t^2), J_{ii} = J_i/(m_t h_t^2),$$
$$h_{ii} = h_i/h_t, m_{ii} = m_i/m_t, A_{ii} = A_i/A_t, q_{ii} = Q_{ii}/Q_{11}^R \text{ and } \breve{q}_{11}^{(i)} = \breve{Q}_{11}^{(i)}/Q_{11}^R \quad (7)$$

where, $T = L\sqrt{m_t/(Q_{11}^R A_t)}$, $h_t = \sum_{i=1}^{3} h_i$, $A_t = \sum_{i=1}^{3} A_i$, $m_t = \sum_{i=1}^{3} m_i$ and Q_{11}^R is the real part of Q_{11}.

Applying the above mentioned adimensional parameters to the equations of motion, Eqs. (3)-(6), and removing the "^" sign, results in four non-dimensionalized equations of motion as:

$$\mathbf{I} \cdot \ddot{u} + \mathbf{L} \cdot u = \mathbf{F} \quad (8)$$

where, $u = [w_1, w_3, u_1, u_3]^T$ in which superscript "T" denotes the transpose of the corresponding matrix. $\mathbf{I, L,}$ and $\mathbf{F}$ are, respectively, linear inertia and stiffness operators and the external force resultant, which, for brevity are not presented in the paper.

b) Galerkin discretization

The frequently employed weighted residual method, called Galerkin discretization approach is implemented to solve the equations of motion. The displacement fields are considered as the combination of the suitable shape functions as:

$$w_i(x,t) = \sum_{j=1}^{n_w^{(i)}} \psi_j^{w(i)}(x)q_j^{w(i)}(t), u_i(x,t) = \sum_{j=1}^{n_u^{(i)}} \psi_j^{u(i)}(x)q_j^{u(i)}(t), i = 1,3 \quad (9)$$

where $\mathbf{q}^{w(1)}(t)$, $\mathbf{q}^{w(3)}(t)$, $\mathbf{q}^{u(1)}(t)$ and $\mathbf{q}^{u(3)}(t)$ are, respectively, the transverse and axial generalized coordinates of the upper and lower face sheets, and $\psi_j^{w(1)}(x)$, $\psi_j^{w(3)}(x)$, $\psi_j^{u(1)}(x)$ and $\psi_j^{u(3)}(x)$ are the *j*th clamped-free linear normal modes of the corresponding Euler-Bernoulli beam and rod, respectively.

Substitution of Eq. (9) into the non-dimensional equations of motion and applying the Galerkin procedure [18] yields:

$$\mathbf{M} \cdot \ddot{\mathbf{q}} + \mathbf{K} \cdot \mathbf{q} = \mathbf{f} \tag{10}$$

where $\mathbf{q} = [\mathbf{q}^{w(1)}, \mathbf{q}^{w(3)}, \mathbf{q}^{u(1)}, \mathbf{q}^{u(3)}]^{\mathbf{T}}$. $\mathbf{M}$ and $\mathbf{K}$ are, respectively, the mass and stiffness matrices and $\mathbf{f}$ is the generalized external force resultant vector. The corresponding eigenvalue problem related to $\mathbf{M}$ and $\mathbf{K}$ matrices delivers the free vibration features including the natural frequencies, loss factors and linear normal modes. The mass and stiffness matrices and the generalized force elements read as:

$$M(k, j) = \int_o^1 \psi_k^{w(1)}[I_{11}(\psi_j^{w(1)})]dx, \, K(k, j) = \int_o^1 \psi_k^{w(1)}[L_{11}(\psi_j^{w(1)})]dx, \, j = 1, ..., n_w^{(1)}$$

$$M(k, j + n_w^{(1)}) = \int_o^1 \psi_k^{w(1)}[I_{12}(\psi_j^{w(3)})]dx, \, K(k, j + n_w^{(1)}) = \int_o^1 \psi_k^{w(1)}[L_{12}(\psi_j^{w(3)})]dx, \, j = 1, ..., n_w^{(3)},$$

$$M(k, j + n_w) = \int_o^1 \psi_k^{w(1)}[I_{13}(\psi_j^{u(1)})]dx, \, K(k, j + n_w) = \int_o^1 \psi_k^{w(1)}[L_{13}(\psi_j^{u(1)})]dx, \, j = 1, ..., n_u^{(1)}, \tag{11}$$

$$M(k, j + n_w + n_u^{(1)}) = \int_o^1 \psi_k^{w(1)}[I_{14}(\psi_j^{u(3)})]dx, \, K(k, j + n_w + n_u^{(1)}) = \int_o^1 \psi_k^{w(1)}[L_{14}(\psi_j^{u(3)})]dx, \, j = 1, ..., n_u^{(3)},$$

$$f(k) = \int_o^1 \psi_k^{w(1)}[F_1]dx, \qquad k = 1, ..., n_w^{(1)},$$

where, $F_1 = \eta^2 h_t / (Q_{11}^R A_t) f_1(x, t)$ and $n_w = n_w^{(1)} + n_w^{(3)}$,

$$M(k + n_w^{(1)}, j) = \int_o^1 \psi_k^{w(3)}[I_{21}(\psi_j^{w(1)})]dx, \, K(k + n_w^{(1)}, j) = \int_o^1 \psi_k^{w(3)}[L_{21}(\psi_j^{w(1)})]dx, \, j = 1, ..., n_w^{(1)}$$

$$M(k + n_w^{(1)}, j + n_w^{(1)}) = \int_o^1 \psi_k^{w(3)}[I_{22}(\psi_j^{w(3)})]dx, \, K(k + n_w^{(1)}, j + n_w^{(1)}) = \int_o^1 \psi_k^{w(3)}[L_{22}(\psi_j^{w(3)})]dx, \, j = 1, ..., n_w^{(3)},$$

$$M(k + n_w^{(1)}, j + n_w) = \int_o^1 \psi_k^{w(3)}[I_{23}(\psi_j^{u(1)})]dx, \, K(k + n_w^{(1)}, j + n_w) = \int_o^1 \psi_k^{w(3)}[L_{23}(\psi_j^{u(1)})]dx, \, j = 1, ..., n_u^{(1)}, \tag{12}$$

$$M(k + n_w^{(1)}, j + n_w + n_u^{(1)}) = \int_o^1 \psi_k^{w(3)}[I_{24}(\psi_j^{u(3)})]dx, \, K(k + n_w^{(1)}, j + n_w + n_u^{(1)}) = \int_o^1 \psi_k^{w(3)}[L_{24}(\psi_j^{u(3)})]dx,$$

$$j = 1, ..., n_u^{(3)}, \qquad f(k + n_w^{(1)}) = \int_o^1 \psi_k^{w(3)}[F_2 = o]dx, \qquad k = 1, ..., n_w^{(3)},$$

$$M(k + n_w, j) = \int_o^1 \psi_k^{u(1)}[I_{31}(\psi_j^{w(1)})]dx, \, K(k + n_w, j) = \int_o^1 \psi_k^{u(1)}[L_{31}(\psi_j^{w(1)})]dx, \, j = 1, ..., n_w^{(1)}$$

$$M(k + n_w, j + n_w^{(1)}) = \int_o^1 \psi_k^{u(1)}[I_{32}(\psi_j^{w(3)})]dx, \, K(k + n_w, j + n_w^{(1)}) = \int_o^1 \psi_k^{u(1)}[L_{32}(\psi_j^{w(3)})]dx, \, j = 1, ..., n_w^{(3)},$$

$$M(k + n_w, j + n_w) = \int_o^1 \psi_k^{u(1)}[I_{33}(\psi_j^{u(1)})]dx, \, K(k + n_w, j + n_w) = \int_o^1 \psi_k^{u(1)}[L_{33}(\psi_j^{u(1)})]dx, \, j = 1, ..., n_u^{(1)}, \tag{13}$$

$$M(k + n_w, j + n_w + n_u^{(1)}) = \int_o^1 \psi_k^{u(1)}[I_{34}(\psi_j^{u(3)})]dx, \, K(k + n_w, j + n_w + n_u^{(1)}) = \int_o^1 \psi_k^{u(1)}[L_{34}(\psi_j^{u(3)})]dx,$$

$$j = 1, ..., n_u^{(3)}, \qquad f(k + n_w) = \int_o^1 \psi_k^{u(1)}[F_3 = o]dx, \qquad k = 1, ..., n_u^{(1)},$$

and

$$M(k + n_w + n_u^{(1)}, j) = \int_o^1 \psi_k^{u(3)}[I_{41}(\psi_j^{w(1)})]dx, \, K(k + n_w + n_u^{(1)}, j) = \int_o^1 \psi_k^{u(3)}[L_{41}(\psi_j^{w(1)})]dx, \, j = 1, ..., n_w^{(1)}$$

$$M(k + n_w + n_u^{(1)}, j + n_w^{(1)}) = \int_o^1 \psi_k^{u(3)}[I_{42}(\psi_j^{w(3)})]dx, \, K(k + n_w + n_u^{(1)}, j + n_w^{(1)}) = \int_o^1 \psi_k^{u(3)}[L_{42}(\psi_j^{w(3)})]dx, \, j = 1, ..., n_w^{(3)},$$

$$M(k + n_w + n_u^{(1)}, j + n_w) = \int_o^1 \psi_k^{u(3)}[I_{43}(\psi_j^{u(1)})]dx, \, K(k + n_w + n_u^{(1)}, j + n_w) = \int_o^1 \psi_k^{u(3)}[L_{43}(\psi_j^{u(1)})]dx, \, j = 1, ..., n_u^{(1)}, \tag{14}$$

$$M(k + n_w + n_u^{(1)}, j + n_w + n_u^{(1)}) = \int_o^1 \psi_k^{u(3)}[I_{44}(\psi_j^{u(3)})]dx, \, K(k + n_w + n_u^{(1)}, j + n_w + n_u^{(1)}) = \int_o^1 \psi_k^{u(3)}[L_{44}(\psi_j^{u(3)})]dx,$$

$$j = 1, ..., n_u^{(3)}, \qquad f(k + n_w + n_u^{(1)}) = \int_o^1 \psi_k^{u(3)}[F_4 = o]dx, \qquad k = 1, ..., n_u^{(3)},$$

4. RESULTS AND DISCUSSION

The frequency response study is the main tool for damage detection analysis and is a practical implement for determination of special dynamics features. Hence, in this section, different scenarios, such as core Young's modulus and the rotary inertia effects on the frequency response are examined.

a) Validation

For validation of the results, the natural frequencies are compared with those of [9]. In [9] a quadratic distribution for transverse displacement is considered along the depth of the core. The beam length and width are, respectively, 36 and 1 *in*. The other properties are presented in Table 1. The results, in Table 2, show that the present results are higher than those of [9]. In agreement with the concluding remarks of [9], which is "*All higher order models are found to compute frequencies which are numerically higher than those of first order theory for the thin beams*", the current results are lower than the corresponding results of [9]. The discrepancy of the transverse frequencies decreases significantly with increasing the mode number (below 10%).

Table 1. Geometric and material properties of isotropic sandwich beam with a flexible core [9]

	Thickness (*in*)	Young's modulus (*psi*)	Shear modulus (*psi*)	Density (lbs^2/in^4)
Upper and Lower face sheets	0.018	10^7	0	250.98×10^{-6}
Core	0.5	0	12000	3.0717×10^{-6}

Table 2. Flapping and axial natural frequencies in comparison with the corresponding results of [9]

	Flapping frequency					Axial frequency	
Mode number	1	2	3	4	5	1	2
Current results(Hz)	25.2	174.9	465.0	865.0	1301.4	1688.33	5070.97
Results from [9] (Hz)	33.7	197.5	505.5	890.5	1321	1648	4941
Percent of difference	25.3	11.4	8.0	2.9	1.5	2.4	2.6

The current frequency response results are compared with those of a beam with viscoelastic core and isotropic face sheets in [5]. In [5], the formulation is based on the MMT assumptions. The assumed mode method has been implemented in [5] to determine the frequency response. The material and geometric properties are presented in Table 3 in which G* is the core complex shear modulus and $f_o = 1 N$. The tip point of the neutral axis of the sandwich beam is considered as the observing point. The results for two core cases, named soft, G*=0.895+1.3067i *MPa*, and hard, G*=9.89+14.4394i *MPa*, are depicted in Fig. 2. A good agreement in prediction of the natural frequencies is evident. In the soft core case, Fig. 2a, the first and second frequencies are predicted less than those of [5], while the third and fourth ones are more than those of [5]. The implication is that in the two lowest frequencies the relaxation of the current model dominates the contributions of the axial and bending core strain energies, while in the third and fourth ones, the core axial and bending strain energies overcome the relaxation of the present model; because the relaxation has a softening effect on the stiffness of the structure, while consideration of the core axial and bending stiffness has a hardening effect on the structural stiffness. In the hard core case, Fig. 2b, the situation is reverse. In the first frequency, the axial and flexural core strain energies dominate the current model relaxation; on the contrary, for the other frequencies the inverse contribution is clear.

Table 3. Geometric and material properties of the isotropic sandwich beam with viscoelastic core [5]

	Thickness (m)	Young's modulus (MPa)	Density (kg/m^3)	Poisson's ratio
Upper face sheet	2×10^{-3}	49×10^3	7500	0.3
Core	1×10^{-3}	$E^* = 2G^*(1+\nu)$	1000	0.49
Lower face sheet	4×10^{-3}	70×10^3	2110	0.3
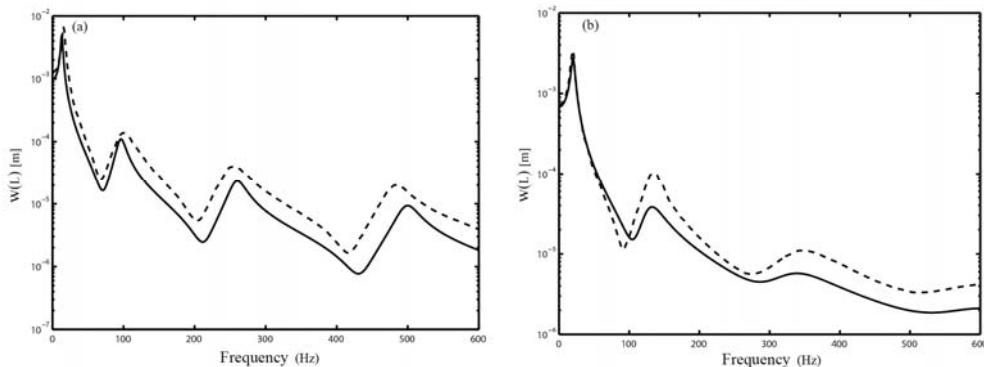
Fig. 2. Frequency response of a clamped sandwich beam with viscoelastic core and isotropic face sheets, (a)- a soft core, G^*=(0.895+1.3067i) MPa, and (b)- a hard core, G^* =(9.89+14.4394i) MPa. The solid and dashed lines indicate, respectively, the current Galerkin approach results and the results of [5]

b) *Frequency response analysis*

In the frequency response analysis of the composite sandwich beams, graphite-epoxy (T300/5208) is considered as the face sheets material. The face sheets and core material properties and the geometric properties are introduced, respectively, in Table 4 and Table 5 and $f_o = 0.1 N$. For more intensive examination, four core cases are considered; the core shear modulus is considered 10^{-1}, 10^0, 10^1 and 10^2 times the reported value in Table 4. The fiber angle study is addressed here. In accordance with the current formulation, which is based on the symmetric layup, the fiber angles of the face sheets are taken the same. The associated frequency response for different fiber angles is displayed in Figs. 3-6. Figure 3 is associated with the weakest core. As expected, increment in the fiber angles has softening effects on the beam stiffness, which reduces the natural frequencies and increases the transverse displacement (more pronounced in 0°-30° fiber angles) while it seems that increasing the fiber angle more than 75° has no significant effect on the corresponding natural frequencies as well as the frequency response. Similar qualitative features are depicted in Figs. 4-6 for the other cases.

Table 4. Material properties of the sandwich beam with viscoelastic core and composite face sheets [14]

	Young's modulus		Density	Poisson's ratio	Shear modulus
	E_{11} (MPa)	E_{22} (MPa)	ρ (kg/m^3)	ν_{12}	G_{12} (MPa)
Upper face sheet	141200	9720	1536	0.28	5530
Core	$E^* = 2G^*(1+\nu)$		970	0.49	$G^* = 7.037(1+0.3i)10^{-1}$
Lower face sheet	141200	9720	1536	0.28	5530

Table 5. Geometric properties of the composite sandwich beam with viscoelastic core [14]

Beam length L(m)	Upper face sheet thickness h_1(m)	Lower face sheet thickness h_3(m)	Core thickness h_2(m)	Beam width b(m)
1	4×10^{-3}	4×10^{-3}	20×10^{-3}	25×10^{-3}
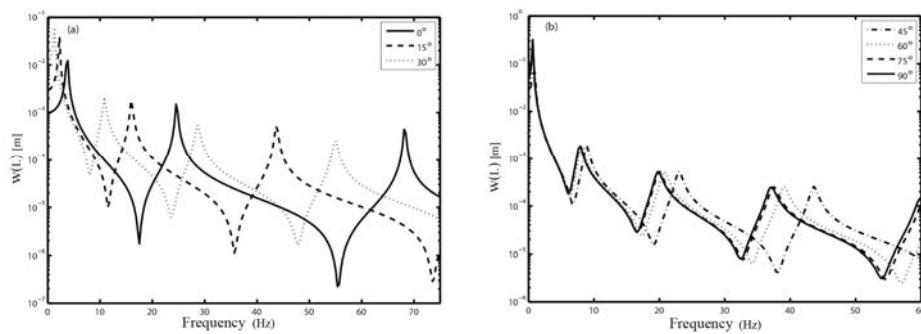
Fig. 3. Frequency response of a clamped sandwich beam with viscoelastic core, $G^*=7.037(1+0.3i)10^{-2}$ *MPa*, and composite face sheets, (a)- face sheets angle equal to: 0°, 15° and 30°, and (b)- face sheets angle equal to: 45°, 60°, 75° and 90°
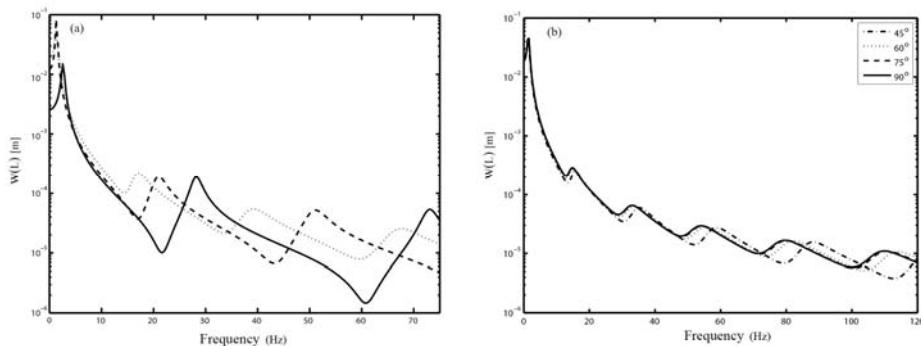
Fig. 4. Frequency response of a clamped sandwich beam with viscoelastic core, $G^*=7.037(1+0.3i)10^{-1}$ *MPa*, and composite face sheets, (a)- face sheets angle equal to: 0°, 15° and 30°, and (b)- face sheets angle equal to: 45°, 60°, 75° and 90°
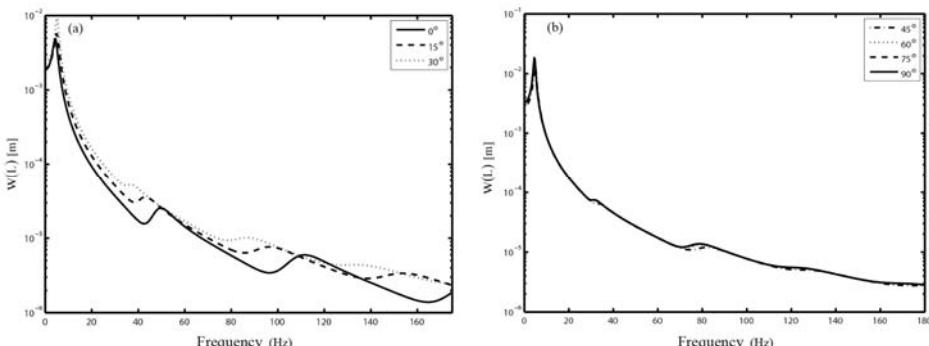
Fig. 5. Frequency response of a clamped sandwich beam with viscoelastic core, $G^*=7.037(1+0.3i)10^{0}$ *MPa*, and composite face sheets, (a)- face sheets angle equal to: 0°, 15° and 30°, and (b)- face sheets angle equal to: 45°, 60°, 75° and 90°
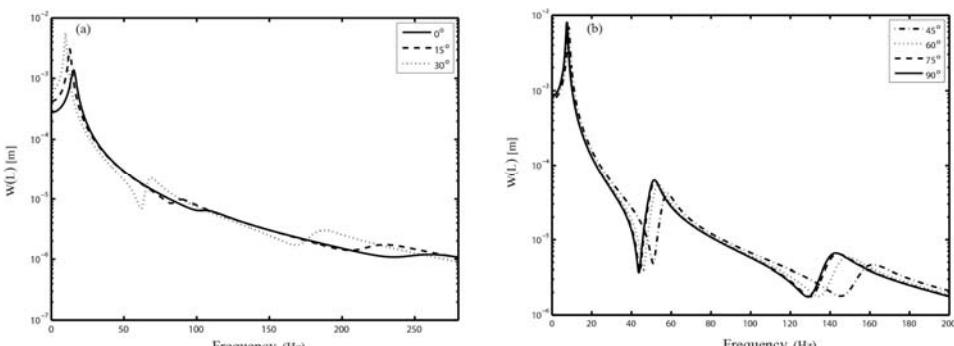
Fig. 6. Frequency response of a clamped sandwich beam with viscoelastic core, $G^*=7.037(1+0.3i)10^{1}$ *MPa*, and composite face sheets, (a)- face sheets angle equal to: 0°, 15° and 30°, and (b)- face sheets angle equal to: 45°, 60°, 75° and 90°

A more interesting study is carried out on the specialized features of the current assumptions and formulation. The two of the more outstanding characteristics of the present formulation are regarding the core Young's modulus, which participates in the axial and flexural strain energies of the core and plays a hardening role in the structural stiffness, and the beam rotary inertia, which affects the beam kinetic energy and softens the structure. The former study is revealed in Figs. 7-9 in which the core shear modulus is considered 10^0, 10^1, 10^2 and 10^3 times the reported value in Table 4. The core thickness is considered, respectively, 1, 2 and 3 times the aforementioned value in Table 5 and the face sheets fiber angles are 30°. The results demonstrate discarding of the core Young's modulus contributions only has obvious influences in the last part, (d), of each figure. On the other hand, the error of the core Young's modulus neglection increases with the core thickness increment.

The implication is that, in part (d) with increasing the core Young's modulus, the core strain energy takes magnitudes in comparison with the face sheet strain energy, hence, discarding the core Young's modulus causes notable errors. In addition, as it is expected, consideration of the core Young's modulus has a hardening effect on the structural stiffness, which is evident in part (d) of each figure.

The rotary inertia effects are investigated in Fig. 10 for 1, 2, 3 and 5 times the previous face sheets thickness value. The face sheets angles and the core shear modulus are considered, respectively, 30° and 10^{-1} times the mentioned value in Table 4. By increasing the face sheets thickness, the rotary inertia effect grows. On the other hand, Fig. 10d exhibits the softening effects of regarding the rotary inertia contributions, which consequently leads to reduction in the natural frequencies.

For more detailed examination of rotary inertia effects, frequency response for the latter case, $h_1=h_3=20\cdot10^{-3}$ m, is depicted in Fig. 11 in which the core shear modulus is considered 10^0, 10^1, 10^2 and 10^3 times the reported value in Table 4.
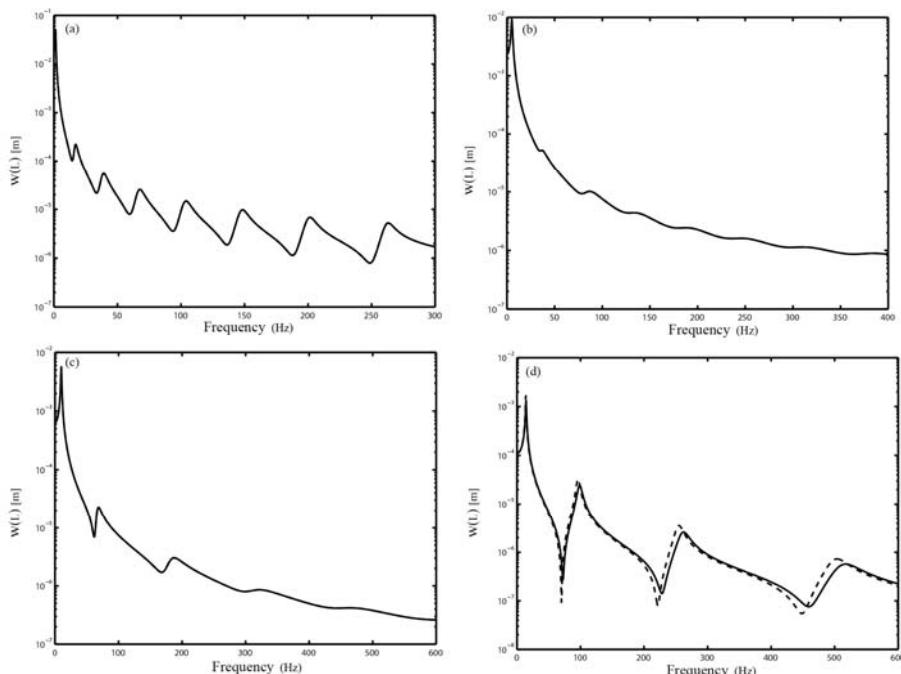
Fig. 7. Frequency response of a clamped sandwich beam with composite face sheets and viscoelastic core with $h_2=2\cdot10^{-2}$ m, (a)- $G^*=7.037(1+0.3i)10^{-1}$ MPa, (b)- $G^*=7.037(1+0.3i)10^0$ MPa, (c)- $G^*=7.037(1+0.3i)10^1$ MPa, and (d)- $G^*=7.037(1+0.3i)10^2$ MPa. The solid and dashed lines indicate, respectively, frequency response with and without the core Young's modulus effects
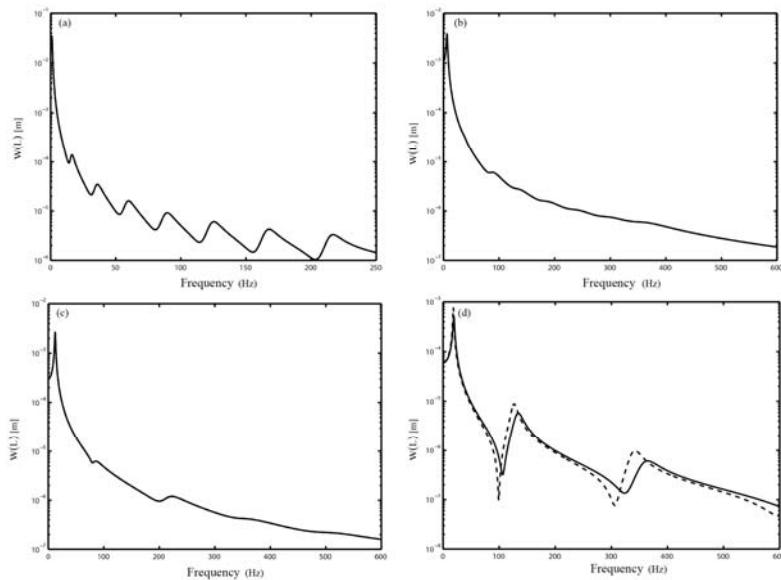
Fig. 8. Frequency response of a clamped sandwich beam with composite face sheets and viscoelastic core with $h_2=4\cdot10^{-2}$ *m*, (a)- $G^*=7.037(1+0.3i)10^{-1}$ *MPa*, (b)- $G^*=7.037(1+0.3i)10^0$ *MPa*, (c)- $G^*=7.037(1+0.3i)10^1$ *MPa*, and (d)- $G^*=7.037(1+0.3i)10^2$ *MPa*. The solid and dashed lines indicate, respectively, frequency response with and without the core Young's modulus effects
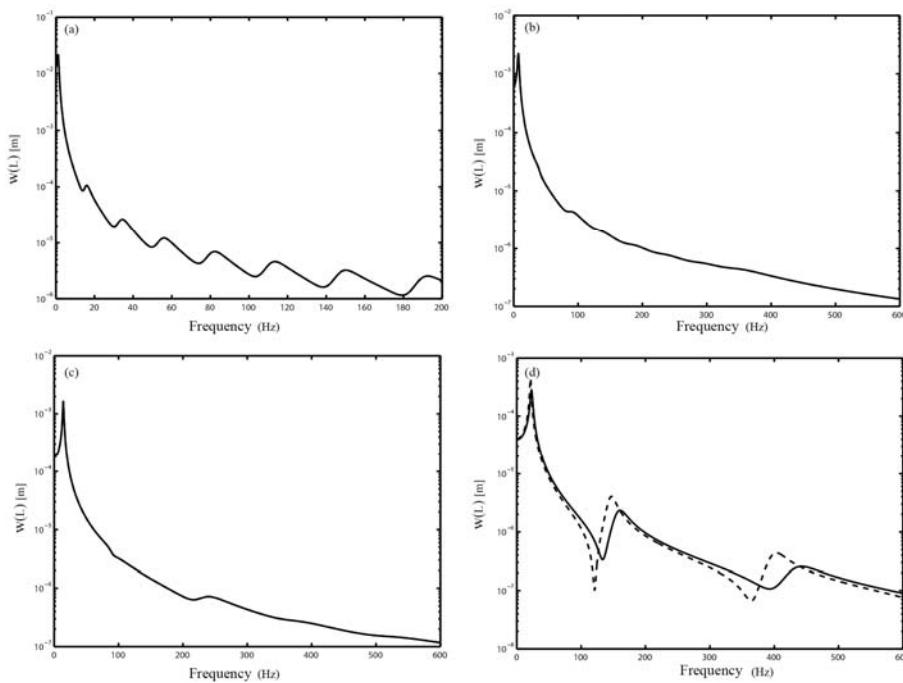
Fig. 9. Frequency response of a clamped sandwich beam with composite face sheets and viscoelastic core with $h_2=6\cdot10^{-2}$ *m*, (a)- $G^*=7.037(1+0.3i)10^{-1}$ *MPa*, (b)- $G^*=7.037(1+0.3i)10^0$ *MPa*, (c)- $G^*=7.037(1+0.3i)10^1$ *MPa*, and (d)- $G^*=7.037(1+0.3i)10^2$ *MPa*. The solid and dashed lines indicate, respectively, frequency response with and without the core Young's modulus effects

The figures demonstrate that core shear modulus increment eliminates the rotary inertia contributions. The implication is that by increasing core Young's modulus magnitude, kinetic energy variation with respect to strain energy variation is negligible. In this case, the rotary inertia influences can be neglected.

The core thickness effects on regarding or discarding of rotary inertia effects is presented in Fig. 12. The core shear modulus and the core thickness are considered, respectively, 10^{-1} and 4 times the corresponding values, respectively, in Tables 4 and 5. In spite of the previous study on the prominent effects of the face sheets thicknesses variation on the frequency response and in agreement with Fig. 10a,

considering rotary inertia effects during the core thickness variation study has no effect on the predicted results.
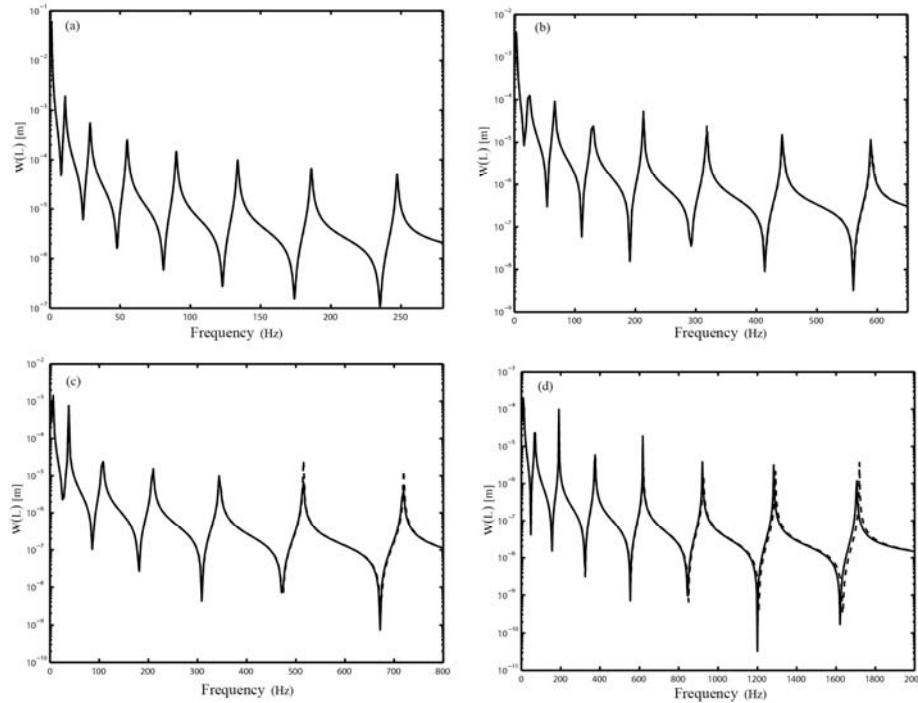
Fig. 10. Frequency response of a clamped sandwich beam with viscoelastic core, $G^*=7.037(1+0.3i)10^{-1}$ *MPa*, and composite face sheets (a)- $h_1=h_3=4\cdot10^{-3}$ *m*, (b)- $h_1=h_3=8\cdot10^{-3}$ *m*, (c)- $h_1=h_3=12\cdot10^{-3}$ *m*, (d)- $h_1=h_3=20\cdot10^{-3}$ *m*. The solid and dashed lines indicate, respectively, frequency response with and without the rotary inertia effects
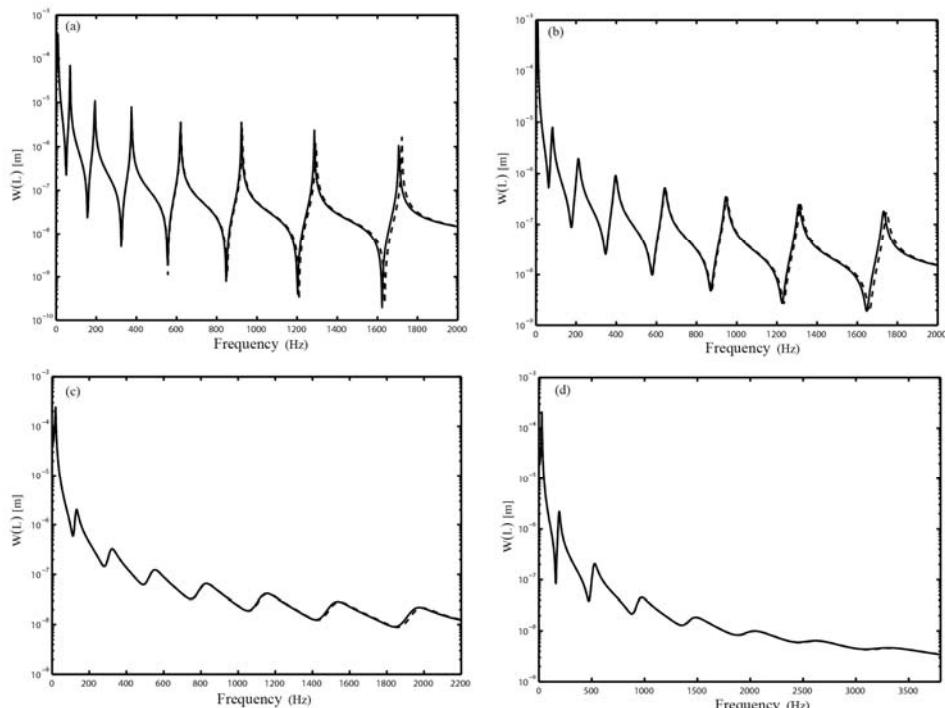
Fig. 11. Frequency response of a clamped sandwich beam with composite face sheets, $h_1=h_3=20\cdot10^{-3}$ *m*, and viscoelastic core, (a)- $G^*=7.037(1+0.3i)10^{-1}$ *MPa*, (b)- $G^*=7.037(1+0.3i)10^{0}$ *MPa*, (c)- $G^*=7.037(1+0.3i)10^{1}$ *MPa*, and (d)- $G^*=7.037(1+0.3i)10^{2}$ *MPa*. The solid and dashed lines indicate, respectively, frequency response with and without the rotary inertia effects
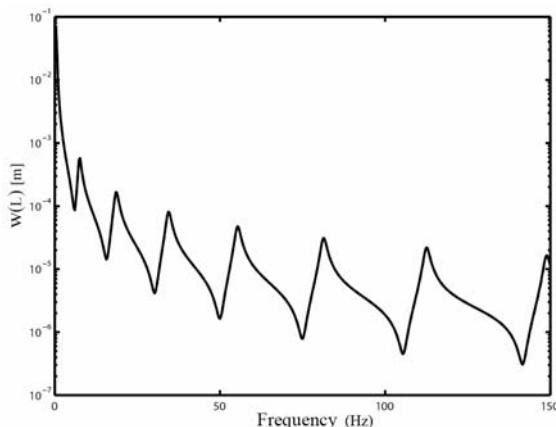
Fig. 12. Frequency response of a clamped sandwich beam with composite face sheets and viscoelastic core, $G^*=7.037(1+0.3i)10^{-2}$ *MPa*, with $h_2=8\cdot10^{-2}$ *m*. The solid and dashed lines indicate, respectively, frequency response with and without the rotary inertia effects

5. CONCLUDING REMARKS

The Hamilton's principle was used to derive the four coupled partial differential equations of motion. The equations of motion were based on the higher order theory of composite sandwich beams, proposed in [14]. The non-dimensional parameters were introduced to find the adimensional forms of the equations of motion. The Galerkin discretization approach was applied on the non-dimensional equations of motion for the frequency response investigation. The face sheets fiber angle and layer thicknesses effects on the frequency response were examined. A very interesting study was established for exploration of the effects of different ratios of the core shear modulus with respect to the face sheets Young's modulus on the frequency response of the beam. The main innovations of this research are summarized as follows: the fiber angles increment makes the structure softer, in other words, it causes a reduction in the natural frequencies and an enlargement in the transverse displacements. A more interesting study was carried out on the specialized features of the current formulation, i.e. regarding the core Young's modulus, which participated in the axial and bending strain energies and hardens the structural stiffness, as it is expected, and the beam rotary inertia, which affects the beam kinetic energy and has a softening effect. The results showed the errors of discarding the core Young's modulus effects are more evident with increasing the core thickness and shear modulus. On the other hand, the rotary inertia effect is manifested by increment in the face sheets thickness, while when the face sheet remains constant it can be neglected in spite of the increment in the core thickness. Hence, for relatively strong shear modulus with respect to the face sheets Young's modulus, the core Young's modulus cannot be neglected, on the other hand, for relatively thick face sheets, elimination of the rotary inertia effects makes evident errors.

REFERENCES

1. Mead, D. J. & Markus, S. (1969). The forced vibration of a three layer, damped sandwich beam with arbitrary boundary conditions. *J Sound Vib*, Vol. 10, No. 2, pp. 163-175.
2. Shakeri, M., Eslami, M. R. & Alibiglu, A. (2002). Analysis of multi-layered shallow panels under dynamic thermal load based on the theory of elasticity. *Iranian Journal of Science Technology Transactions of Mechanical Engineering*, Vol. 26, No. 3, pp. 441-454.
3. Yim, J. H., Cho, S. Y., Seo, Y. J. & Jang, B. Z. (2003). A study on material damping of 0° laminated composite sandwich cantilever beams with a viscoelastic layer. *Compos Struct*, Vol. 60, pp. 367-374.

4. Pourtakdoust, S. H. & Fazelzadeh, S. A. (2003). Effect of structural damping on chaotic behavior of nonlinear panel flutter. *Iranian Journal of Science Technology Transactions of Mechanical Engineering*, Vol. 27, No. 3, pp. 453-467.

5. Cai, C., Zheng, H. & Liu, G. R. (2004). Vibration analysis of a beam with PCLD patch. *Appl Acoust*, Vol. 65, pp. 1057-1076.

6. Zhang, S. H. & Chen, H. L. (2006). A study on the damping characteristics of laminated composites with integral viscoelastic layers. *Compos Struct*, Vol. 74, pp. 63-69.

7. Douglas, B. E. & Yang, J. C. S. (1978). Transverse compressional damping in the vibratory response of elastic-viscoelastic-elastic beams. *AIAA J*, Vol. 16, No. 9, pp. 925-930.

8. Frostig, Y. & Baruch, M. (1994). Free vibrations of sandwich beams with a transversely flexible core: A high order approach. *J Sound Vib*, Vol. 176, No. 2, pp. 195-208.

9. Marur, S. R. & Kant, T. (1996). Free vibration analysis of fiber reinforced composite beams using higher order theories and finite element modeling. *J Sound Vib*, Vol. 194, No. 3, pp. 337-351.

10. Chen, Q. & Chan, Y. W. (2000). Integral finite element method for dynamical analysis of elastic-viscoelastic composite structures. *Comput Struct*, Vol. 74, pp. 51-64.

11. Douglas, B.E. (1986). Compressional damping in three-layer beams incorporating nearly incompressible viscoelastic cores. *J Sound Vib*, Vol. 104, No. 2, pp. 343-347.

12. Johnson, C.D. (1995). Design of passive damping systems. ASME 50th Anniversary of the Design Engineering Division, *J Mech Des Vib Acoust*, Vol. 117, pp. 171-176.

13. Austin, E. M. & Inman, D. J. (1997). Studies on the kinematics assumptions for sandwich beams. *In Proceedings of SPIE Smart Structures and Materials, LP Davis, Passive Damping and Isolation*, SPIE Vol. 3045, pp. 173-183.

14. Arvin, H., Sadighi, M. & Ohadi, A. R. (2010). A numerical study of free and forced vibration of composite sandwich beam with viscoelastic core. *Compos Struct*, Vol. 92, No. 4, pp. 996-1008.

15. Afshin, M., Sadighi, M. & Shakeri, M. (2011). Vibration and damping analysis of cylindrical sandwich panels containing a viscoelastic flexible core. *J Sandw Struct Mater*, Vol. 13, No. 3, pp. 331-356.

16. Damanpack, A. R. & Khalili, S. M. R. (2012). High-order free vibration analysis of sandwich beams with a flexible core using dynamic stiffness method. *Compos Struct*, Vol. 94, No. 5, pp. 1503-1514.

17. Venkatachalam, R., Balasivanandha Prabu, S. & Venkatesh Raja, K. (2012). Finite element based investigation on vibrational performance of a sandwich system. *J Vib Control*, Vol. 18, No. 9, pp. 1284-1290.

18. Meirovitch, L. (1997). *Principles and techniques of vibrations*. New York, McGraw Hill.